

# Elasticity Imaging of the Lung with Fuzzy Control-Based Image Registration Using Multidetector-Row CT

Syoji Kobashi\*, Yosuke Yanagida, Katsuya Kondo, and Yutaka Hata  
University of Hyogo, Graduate School of Engineering, JAPAN

Received 14 November 2006; accepted 9 March 2007

---

## Abstract

Pulmonary diseases of the lung often cause the change of elasticity. This article proposes a novel elasticity imaging method using multidetector-row CT (MDCT). The new method is based on non-rigid image registration from MDCT images of the inspiratory lung to those of the expiratory lung. The elasticity is calculated by local volume change between respirations. Also, this article introduces a new image registration method based on a fuzzy control system. The fuzzy control deforms the given image according to knowledge on density of lung vessels, shape, and anatomical structure. The proposed elasticity imaging method was evaluated using computer synthetic data and subjects' data. The experimental results showed that the proposed method deformed the given image successfully, and estimated the relative elasticity with a correlation coefficient of 0.86.

## Keywords

Lung elasticity imaging, Multidetector-row CT, Non-rigid image registration, Fuzzy control

---

## 1. INTRODUCTION

Multidetector-row computed tomography (MDCT) can provide sectional images that have high spatial resolution at a short acquisition time. However, an increase of MDCT images makes manual diagnosis tedious and extremely time-consuming. Therefore, a computer-aided diagnosis (CAD) system for chest MDCT images has been attracting considerable attentions. There are conventional studies on the CAD system [1][2][3]. For example, bronchus extraction [4][5], detection of lung nodules [6][7], and analysis of diseased regions [8] have been studied. These studies support us to diagnose pulmonary diseases and to understand lung anatomy.

Human lung is an organ which exchanges gas with external world by repeating expansion and shrinkage. By comparing MDCT images of the inspiratory lung with those of the expiratory lung, we can see that the lung is widely deformed. Expansion and shrinkage of the healthy lung are induced uniformly. But in case of the diseased lung such as idiopathic interstitial pneumonia (IIP) [9], they might be induced non-uniformly because walls of the lung alveoli become thick due to plutonic inflammation. As a result, uniform expansion and shrinkage is interfered. In that case, it seems that the diseased part is stiffer than other parts. Therefore, the elasticity imaging can reveal the difference

of the stiffness and can support us to diagnose the pulmonary diseases.

In general, tissue elasticity has been measured by using ultrasonic wave [10]. The measurement techniques can be roughly classified into a dynamic technique [11][12] and a static technique [13][14]. The dynamic technique is performed by analyzing the response of tissues to a low frequency wave. The induced displacement by the low frequency wave is measured by Doppler ultrasound technique where the displacement is determined by time-delay estimation methods between signals at a low compression level and at a high compression level [12]. The static technique is based on external tissue compression with subsequent computation of the strain, which is derived from cross-correlation analysis between acquired ultrasonic waves of pre- and post-compressions. The strain can be converted into an elastic modulus by measuring the applied stresses [13][14]. These tissue elasticity imaging systems are effective for analyzing soft tissues located near the body surface. In other words, they cannot be applied to the pulmonary tissues because the lung is fulfilled with air and almost power of ultrasound is reflected at the boundary of the lung.

\* Syoji Kobashi; University of Hyogo, Graduate School of Engineering; 2167, Shosha, Himeji, Hyogo, 671-2280, JAPAN; Phone/Fax + 81-79-267-4989; kobashi@eng.u-hyogo.ac.jp

This article proposes a novel lung elasticity imaging method using MDCT. The method estimates local relative elasticity of the lung by calculating local volume change between respirations. The local volume change can be measured by acquiring MDCT images of the inspiratory lung and of the expiratory lung from the same subject and by finding corresponding points between respirations. Thus, elasticity estimation can be performed with non-rigid image registration of MDCT images.

Many image registration algorithms have been reported [15]. Especially, Park *et al.* showed a method for chest MDCT images [16]. This method first extracts bronchial tree from MDCT images, and then finds corresponding branching point by using a graph matching algorithm. The limitation of this method is that it is difficult to find corresponding points at the tail of bronchi because artifacts or spatial limitation of MDCT scanner makes it difficult to extract thin bronchi. Furthermore, the reliability of the displacement vector decreases with increasing the distance from the bronchial tube.

Thus, this article proposes a new image registration method for MDCT images of the lung between respirations. The inspiratory lung should have the same branch structure as the expiratory lung. Therefore, spatial distribution of vessel density of the expiratory lung should be similar to that of the inspiratory lung. The proposed method is implemented based on a fuzzy control system. The fuzzy control deforms the given MDCT images so that the spatial distribution of vessel density is similar to that of target images. A part of this paper was appeared in Ref. [17].

## 2. MATERIALS

We acquired MDCT images with an MDCT scanner (LightSpeed Ultra 16; GE Medical Systems, Milwaukee, WI). Field of view was 360 by 360 mm, matrix was 512 by 512 pixels, and thickness of slices was 0.625 mm. The volume data including from the apex of the lung to the diaphragmatic surface were composed of over than 400 slices. An example of MDCT image is shown in Figure 1. Because the lung and the outside body regions are filled by air, CT values stored in the voxels were about -800 HU (Hounsfield Units) and they were appeared as dark gray in MDCT images. And CT values stored in voxels of the other regions such as bone, fat and muscle were between 0 and 1000 HU, and they were appeared as white in images. For each subject who was employed in this study, a pair

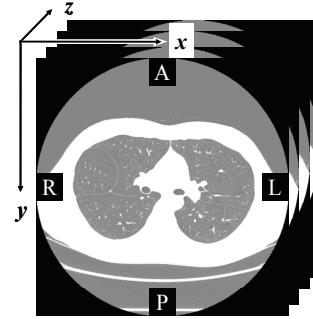


**Figure 1. An example of MDCT image. A; anterior, P; posterior, R; right, L; left.**

of inspiratory and expiratory MDCT images was acquired. During taking MDCT images (about 15 sec), the subject was instructed to hold his breath.

## 3. LUNG ELASTICITY ESTIMATION USING MDCT

Human lung repeats expansion and shrinkage for the purpose of gas exchanging. In this process, soft part of the lung will expand and shrink greatly, and hard part will expand and shrink gently. Therefore, local elasticity can be estimated by calculating local volume change of MDCT images between the inspiratory lung and the expiratory lung. This study calculates the local volume change by image registration of MDCT images from the inspiratory lung to the expiratory lung.

### Preprocessing

From each of inspiratory and expiratory MDCT images, the method first segments the lung region. We define the lung region as air region excluding bronchial region and have smooth curved surface that doesn't have holes or lacks. Since the air region appears with a low CT value in MDCT images, the air region in the lung can be segmented by 3-D region growing. The bronchial region is enclosed by the bronchial wall which has higher CT value than that of the air region. The lung region is segmented by excluding the bronchial region from the air region. The segmented lung region has many holes and lacks around hilum of lung. Because they have higher intensity than air, they can be filled by morphology closing methods and then obtain the smooth curved lung region.

Next, blood vessels and bronchial wall are segmented by threshold processing because blood vessels and bronchial wall have high intensity in the segmented lung region. Then, the segmented lung region is decomposed into five lung lobes (left upper and lower lobes, right upper middle and lower lobes) using our previously developed

method [18], which segments the lung lobes by finding the boundary surfaces based on the distribution of tubular tissues and lobar fissures.

### Image registration with fuzzy control

#### Assign nodes

The segmented inspiratory lung is converted into a lattice structure whose distance between neighboring intersecting-points (*i.e.*, nodes) is  $L_0$  (15 mm was used in this study). The lattice structure constructed by nodes is the initial form to be deformed. The following registration processes are performed by updating the positions of the nodes.

#### Calculate features

Nodes are moved by a fuzzy control system so that the deformed inspiratory lung region is equal to the expiratory lung. For each node, fuzzy control system works with respect to three features ( $\mathbf{VD}$ ,  $\mathbf{S}$ , and  $\mathbf{L}$ ) of a node with a coordinate value of  $\mathbf{P}; [x, y, z]^T$ .

The first feature  $\mathbf{VD} = [VD_x, VD_y, VD_z]^T$  evaluates similarity between the deforming inspiratory lung region and the expiratory lung with respect to a gradient vector, and it is calculated by;

$$\mathbf{VD} = \nabla(\nabla(D_{ins}) \otimes \nabla(D_{ex})), \quad (1)$$

where  $D_{ins}$  and  $D_{ex}$  are the vessel densities [ $\text{mm}^3 / 10^3 \text{ mm}^3$ ] calculated from MDCT images of the inspiratory lung and the expiratory lung, respectively. And,  $\nabla(\mathbf{A})$  is an operation to calculate the gradient vector of  $\mathbf{A}$ , and  $\mathbf{A} \otimes \mathbf{B}$  is an operation to calculate inner product by convoluting  $\mathbf{A}$  into  $\mathbf{B}$  with translating  $\mathbf{A}$ . The smaller norm of  $\mathbf{VD}$  means that the gradient of density of the expiratory lung is similar to that of the deforming lung. And, the direction of  $\mathbf{VD}$  shows the direction where the node of interest should be moved.

The second feature  $\mathbf{S} = [S_x, S_y, S_z]^T$  evaluates spatial smoothness around the node of interest. It is defined as a vector from a gravity point of the six neighboring nodes. The norm of  $\mathbf{S}$  becomes the lower value when the 3-D shape around the node of interest becomes smooth. And, the direction of  $\mathbf{S}$  shows the direction where the node of interest should be moved.

The third feature  $\mathbf{L} = [L_x, L_y, L_z]^T$  evaluates whether the node of interest belongs to the correct lung lobe. For example, when a node belongs to the right upper lobe during inspiration, the node should

belong to the right upper lobe during expiration.  $\mathbf{L}$  [mm] is a vector from the node of interest to the nearest voxel of the correct lung lobe, which is defined by;

$$\mathbf{L} = \begin{cases} 0 & \text{if label}(\mathbf{P}) = L_t \\ \mathbf{Q} - \mathbf{P} & \text{others} \end{cases} \quad (2)$$

$$\mathbf{Q} = \arg \text{MIN}_{\text{label}(\mathbf{Q})=L_t} [\delta(\mathbf{Q}, \mathbf{P})], \quad (3)$$

where  $\text{label}(\mathbf{P})$  is the label of the lung lobe at coordinate value  $\mathbf{P}$  in the MDCT images of the expiratory lung,  $L_t$  is the label of the lung lobe of the node of interest in the MDCT images of the deforming expiratory lung lobe.  $\mathbf{Q}$  is coordinate value of the nearest voxel to the node of interest and is belonging to the correct lobes, and  $\delta(\mathbf{A}, \mathbf{B})$  is Euclidean distance between point  $\mathbf{A}$  and  $\mathbf{B}$ .

These three feature vectors ( $\mathbf{VD}$ ,  $\mathbf{S}$  and  $\mathbf{L}$ ) are calculated for each node, and updated for each iteration. And, their norms are divided by normalization parameters,  $\alpha_{VD}$ ,  $\alpha_S$ , and  $\alpha_L$ , respectively.

#### Move Nodes by Fuzzy Control

Fuzzy control is a system for estimating moving vector of a node,  $\mathbf{T} = [T_x, T_y, T_z]^T$ . It calculates moving distance of the node for each axis. The followings show the fuzzy control system along  $x$ -axis for a node, and fuzzy control of the other axes can be achieved in the same way.

1. **Fuzzy Linguistics:** To describe the magnitude of features of the node, three fuzzy linguistics,  $N$ ,  $Z$ , and  $P$ , are defined by fuzzy membership functions shown in Figure 2. And, to describe the magnitude of  $x$ -component of moving vector of the node, five fuzzy linguistics,  $NB$ ,  $NM$ ,  $Ze$ ,  $PM$ , and  $PB$ , are defined by fuzzy membership functions shown in Figure 3.
2. **Fuzzy Rules:** 27 fuzzy rules are defined as shown in Table 1 to determine the behavior of the fuzzy control system. For example, one cell can be interpreted into

$$\begin{array}{l} \text{IF } (VD_x \text{ is } N) \text{ AND } (L_x \text{ is } Z) \\ \text{AND } (S_x \text{ is } N) \text{ THEN } (T_x \text{ is } NB) \end{array}$$

This fuzzy rule table is designed to give the higher dependency on the feature value  $L_x$  in comparison with the other feature values so that nodes keep belonging to the correct region. When the node belongs to the correct lobe, the moving distance of the node is determined primarily by the remained feature values  $VD_x$

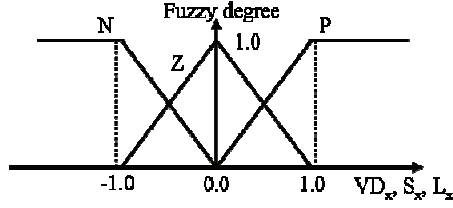


Figure 2. Membership functions of fuzzy linguistics to describe features of node.

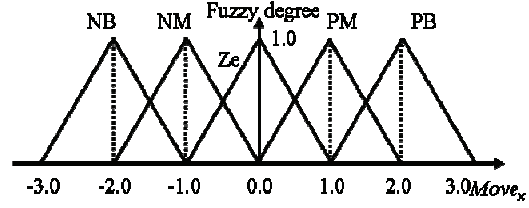


Figure 3. Membership functions of fuzzy linguistics to describe moving distance.

Table 1. Fuzzy rule table for image registration of lung MDCT images.

	$L_x=N$	$L_x=Z$			$L_x=P$
$S_x=N$	NB	NB	NM	Ze	PB
$S_x=Z$		NM	Ze	PM	
$S_x=P$		Ze	PM	PB	

and  $S_x$ . Fuzzy rules in  $y$ - and  $z$ -axes are also designed with the same manner as those in  $x$ -axis.

The  $x$ -component of moving vector,  $T_x$ , is obtained by using Mamdani's min-max and center of gravity method [19]. In the same way, moving distances for  $y$ - and  $z$ -axes are obtained. This fuzzy control process is applied to all nodes, and after calculating moving vectors of all nodes, the nodes are moved by the calculated moving vectors simultaneously. The above processes are iterated until the summation of the moving vectors' norms of the all nodes becomes less than a convergence parameter  $\delta_{min}$ . In summary, fuzzy control based image registration algorithm is performed with the following steps.

- (Step 0) Calculate vessel density of the expiratory lung. And, convert the inspiratory lung region to be deformed into lattice structure representation.
- (Step 1) Calculate vessel density at every node of the deforming lung, and extract three features for every node.
- (Step 2) Calculate moving vector for every node using the fuzzy control system.
- (Step 3) Move all nodes by the calculated moving vector.
- (Step 4) If the summation of norms of moving vectors is less than  $\delta_{min}$ , terminate this procedure, otherwise go to step 1.

### Elasticity estimation using local volume change

In general, bulk modulus,  $K$ , of a solid is estimated by stressing the solid from the surface with the arbitrary pressure, and it is defined as;

$$K = -V \left[ \frac{\partial P}{\partial V} \right]_T, \quad (4)$$

where  $V$  is volume before stressing,  $P$  is pressure and subscript  $T$  indicates that the partial differential is calculated at constant temperature. To calculate relative bulk modulus  $K$  of a part of the solid, we assume that pressure  $P$  is constant for every part of the solid. This assumption derives the following equation from Eq. (4).

$$K = -V_0 \left[ \frac{1}{V_I - V_0} \right]_T, \quad (5)$$

where  $V_0$  is the volume of the part before stressing and  $V_I$  is the volume of the deformed part after stressing.

Eq. (5) indicates that we should measure volumes of a part of the lung region before and after stressing to calculate the local elasticity of the lung tissue. Image registration of MDCT images from of the inspiratory lung to of the expiratory lung produces corresponding nodes between the deforming lungs with respiratory. Thus, by calculating volume of hexahedron whose apexes are nodes, we can measure volumes of corresponding hexahedrons and calculate the local volume change with respiratory. According to Eq. (5), local elasticity of the lung tissue is defined as

$$\Delta K = -\Delta V_I \left( \frac{1}{\Delta V_E - \Delta V_I} \right), \quad (6)$$

where  $\Delta K$  is the relative elasticity of the hexahedron.  $\Delta V_I$  and  $\Delta V_E$  are volumes of the hexahedrons in the inspiratory lung and in the expiratory lung, respectively.  $\Delta K$  takes a value higher than 1.0, and almost 1.0 indicates that the hexahedron of

interest is very soft because the volume of the expiratory lung  $\Delta V_E$  becomes almost zero, while the harder tissue gives the higher  $\Delta K$ . This equation is applied to every hexahedron in the lung, and then elasticity map of the lung is obtained.

#### 4. EXPERIMENTAL RESULTS

To evaluate the accuracy of estimating elasticity with the proposed method, it was examined by computer simulation experiment. Materials of this experiment are MDCT images of the inspiratory lung of a normal healthy male subject (23 years old) and computer synthetic MDCT images that were generated by applying affine transform to the MDCT images of the inspiratory lung. The synthetic MDCT images were used as MDCT images of the expiratory lung in the method. The affine matrix used was

$$\begin{bmatrix} x' \\ y' \\ z' \\ 1 \end{bmatrix} = \begin{bmatrix} 1/t & 0 & 0 & c_x \\ 0 & 1/t & 0 & c_y \\ 0 & 0 & 1 & 0 \\ 0 & 0 & 0 & 1 \end{bmatrix} \begin{bmatrix} x - c_x \\ y - c_y \\ z \\ 1 \end{bmatrix} \quad (7)$$

$$\text{and } t = \frac{z}{2(z_I - z_s)} \quad (8)$$

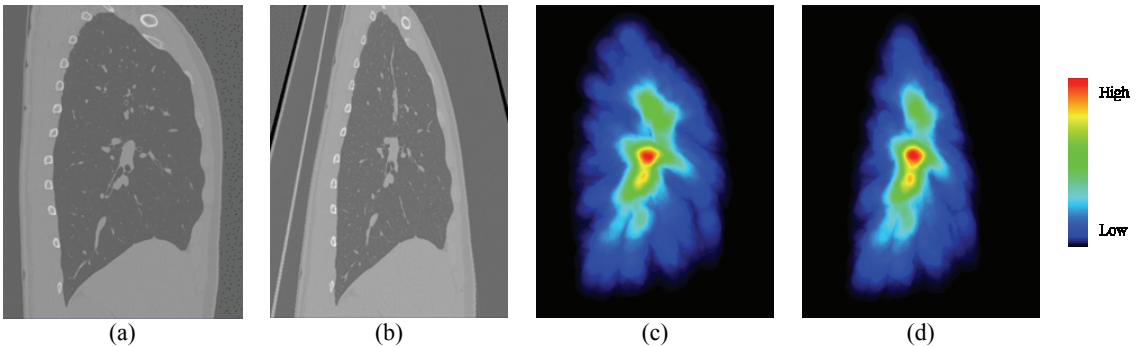
where  $[x, y, z]^T$  is a coordinate value in MDCT images of the inspiratory lung,  $[x', y', z']^T$  is a coordinate value of synthetic MDCT image, and  $c_x$  ( $= 180$ ) and  $c_y$  ( $= 256$ ) are arbitrarily determined point so that the origin of this transformation be the center axis of the left lung. And  $t$  was a shrinking rate,  $z_I$  and  $z_s$  are  $z$ -coordinate value of the most inferior part (apex) and the most superior part (diaphragmatic surface) of the lung, respectively. Figure 4 (a) and (b) show sagittal images of MDCT images of the inspiratory lung and of computer synthesized expiratory lung, respectively. As

shown in these images, this transformation shrink MDCT image greatly with the superior position of the lung.

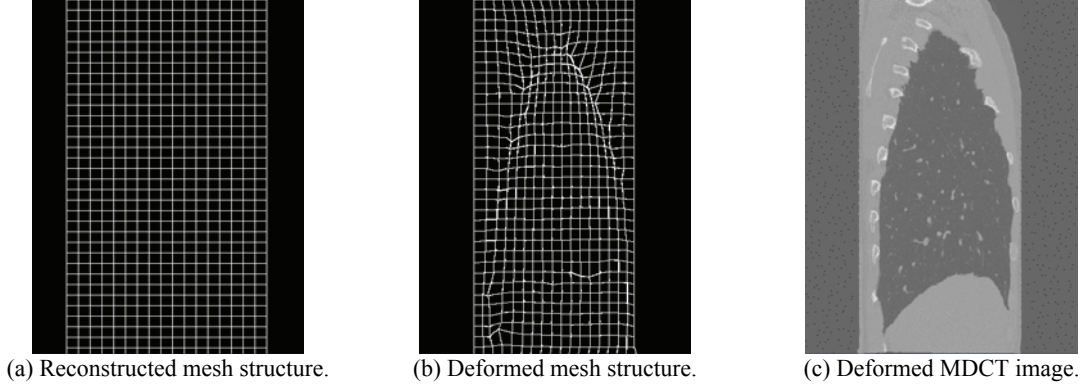
Fuzzy control based image registration of the proposed method was applied to transform Figure 4 (a) into Figure 4 (b). The parameters,  $\alpha_{VD}$ ,  $\alpha_S$ , and  $\alpha_L$ , used were 1.91, 1.67, and 1.67, respectively, that were determined experimentally. Figure 4 (c) and (d) show vessel density map of Figure 4 (a) and (b), respectively. Comparison of them shows that spatial distribution of vessel density was similar. The proposed method first converted the segmented lung region into lattice structure as shown in Figure 5 (a). Figure 5 (b) shows the reconstructed lattice structure after image registration. By deforming Figure 4 (a) according to the deformed lattice structure, the deformed MDCT images as shown in Figure 5 (c) were obtained.

Figure 6 shows absolute-subtraction images of MDCT images of the inspiratory lung from synthetic MDCT images pre- and post- image registration. They show that subtraction image becomes the darker images by applying image registration, and hold that the image registration works well. The computation time for image registration was approximate 5 hours using a computer (CPU: 3.0 GHz, Memory 2 GByte, Linux).

Relative elasticity for each hexahedron was calculated and stored into voxel-space. A sagittal image of the relative elasticity images is shown in Figure 7. This image shows relative elasticity with a color-scale representation (blue-yellow-red). Because computer synthetic images were generated by shrinking the superior part of the lung hardly, the superior position should take the lower relative elasticity (*i.e.*, the superior portion is the softer tissue). The obtained elasticity map shown in Figure 7 agreed with the fact, and it shows that the proposed method calculated relative elasticity successfully.



**Figure 4. Computer simulation experiments; (a) and (b): inspiratory and computer synthesized expiratory MDCT data, (c) and (d): vessel density map of (a) and (b), respectively.**



**Figure 5. Deformation with fuzzy control based image registration.**

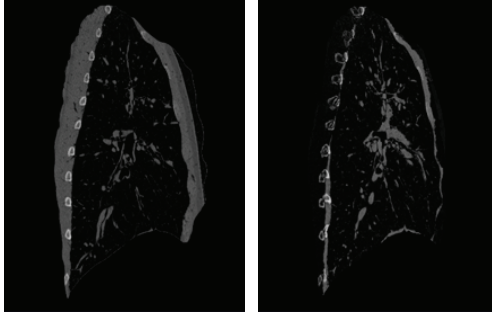


**Figure 6. Subtraction of MDCT images from the inspiratory lung to the synthesized expiratory lung. (left) pre-registration: (right) post-registration.**

The estimated relative elasticity was evaluated by comparing with ground truth data, which was calculated by

$$\Delta K = -\Delta V_l \left( \Delta V_l - \frac{1}{t^2} \Delta V_l \right)^{-1} = \frac{t^2}{t^2 - 1}, \quad (9)$$

according to Eq. (7) and (8). Figure 8 shows the comparison of the estimated relative elasticity with the grand truth data. The estimated elasticity value was deeply correlated with the grand truth value and correlation coefficient was 0.86.

Next, the proposed method was applied to two subjects who were healthy male volunteers (subject 1; 23 years old, and subject 2; 24 years old) with no smoking history. Figure 9 show multiplanar reconstruction (MPR) images that are composed of axial, coronal, and sagittal images, of subject 1 and 2. The images show that the proposed method can be applied to both of subjects. And, as shown in Figure 10, elasticity images were produced successfully. As shown in the elasticity images, the inferior portion of the lung has the lower relative elasticity. This result agrees with the fact that the lower lobes have a lot of vital capacity.

## 5. CONCLUSIONS

Elasticity imaging of the lung can be one of the powerful diagnosing tools of pulmonary diseases. This paper has proposed a novel elasticity imaging method using MDCT. The method is based on image registration that deforms MDCT images of the inspiratory lung into those of the expiratory lung where the MDCT images both of the inspiratory lung and expiratory lung are acquired from the same subject. Then, tissue elasticity is estimated from local volume changes between respirations that are calculated from the results of image registration. The image registration method proposed in this paper is based on fuzzy control, which deforms the given image with respect to vessel density, shape and anatomical structure.

The proposed method was numerically evaluated by applying it to computer synthetic MDCT images. The experiments showed that the proposed method estimated the relative elasticity with strong correlation with the ground truth relative elasticity calculated theoretically. The correlation coefficient between them was 0.86. Also, the method was applied to subjects' data, and the results showed that the local relative elasticity of the inferior lung lobes takes the lower value in comparison with that of the superior lung lobes that are agreed with anatomical experimental knowledge.

There are few limitations of the proposed method. One is a computation time for image registration. To estimate tissue elasticity of more small volumes, we should shorten the computation time for feature extraction of nodes. The other is performance of image registration; there are still some errors of image registration around the center of lung lobes because vessel density of the voxels has a similar value and it decreases the gradient of vessel density.

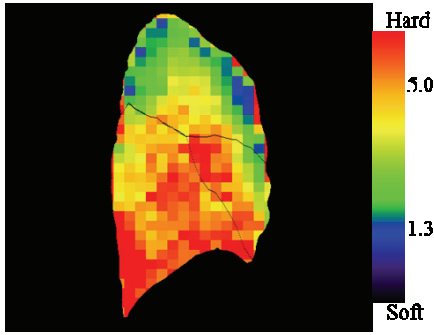


Figure 7. Elasticity image calculated from Figure 5.

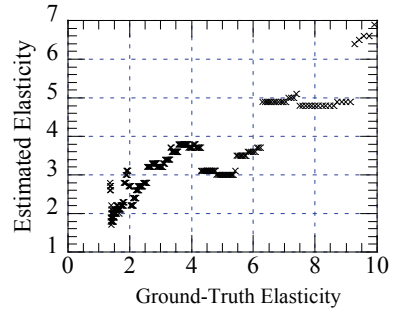


Figure 8. Comparison of estimated elasticity and ground-truth elasticity. Each cross represents the mean relative elasticity in each axial image.

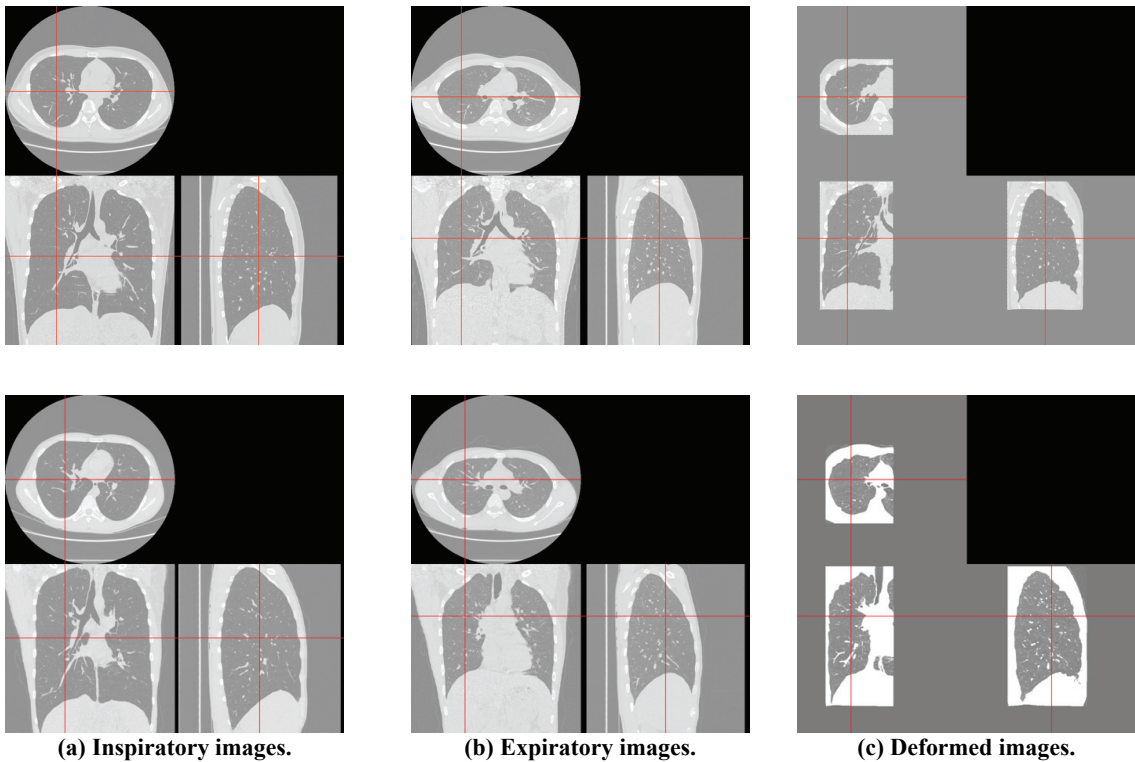


Figure 9. Experimental results of image registration. Upper images: subject 1, Lower images: subject 2. Red lines show the corresponding slices.

In the future, we will introduce the combination of trachea tree matching for more precise registration [15][16] that will be suitable for finding global corresponding between images. After applying the trachea tree matching, our proposed method will deform the images more precisely. Also, we will perform numerical evaluations to evaluate the correlation between estimated local elasticity and that measured by another system such as ultrasonic

systems with *in vitro* study. Then, we will examine the effectiveness of the proposed method in the clinical study.

#### ACKNOWLEDGEMENTS

This research was supported in part by the Ishikawa Hospital Grant, and the BISC (Berkeley Initiative Soft Computing) Program of university of California at Berkeley.

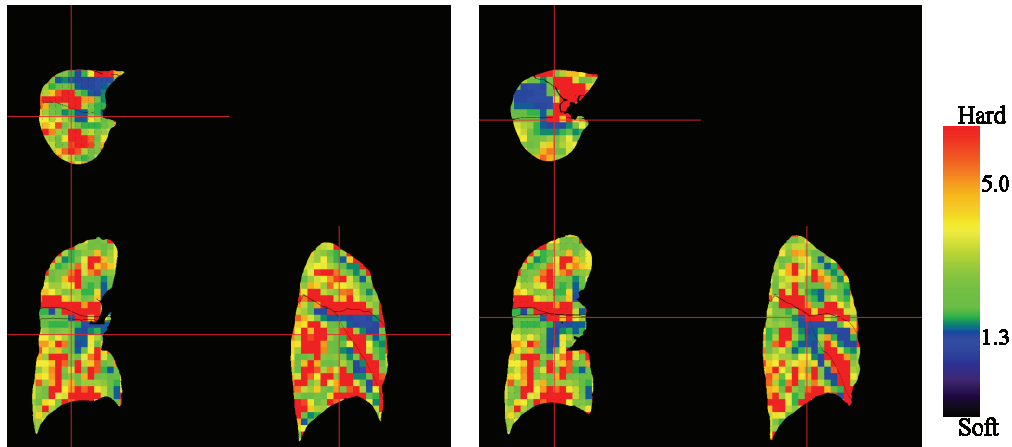


Figure 10. Elasticity images of normal subject 1 (left) and 2 (right).

## REFERENCES

- [1] I. Sluimer, A. Schilham, M. Prokop, and B. van Ginneken, "Computer analysis of computed tomography scans of the lung: a survey," *IEEE Trans. on Med. Imaging*, Vol. 25, No. 4, pp. 385-405, 2006.
- [2] M. N. Mughal and W. Ikram, "Early lung cancer detection by classifying chest CT images: a survey," *Proc. of 8th Int. Multi-topic Conf.*, pp. 67-72, 2004.
- [3] D. M. Hansell, "Imaging the lungs with computed tomography," *IEEE Engineering in Medicine and Biology Magazine*, Vol. 19, No. 5, pp.71-79, 2000.
- [4] K. Mori, J. Hasegawa, Y. Suenaga, and J. Toriwaki, "Automated Anatomical Labeling of the Bronchial Branch and its Application to the Virtual Bronchoscopy System," *IEEE Trans. on Med. Imaging*, Vol. 19, No. 2, pp. 103-114, 2000.
- [5] D. Aykac, E. A. Hoffman, G. McLennan, and J. M. Reinhardt, "Segmentation and Analysis of the Human Airway Tree From Three-Dimensional X-Ray CT Images," *IEEE Trans. on Med. Imaging*, Vol. 22, No. 8, pp. 940-950, 2003.
- [6] M. N. Gurcan, B. Sahiner, N. Petrick, H. Chan, E. A. Kazerooni, P. N. Cascade, and L. Hadjiiski, "Lung Nodule Detection on Thoracic Computed Tomography Images: Preliminary Evaluation of a Computer-aided Diagnosis System," *Medical Physics*, Vol. 29, No. 11, pp. 2552-2558, 2002.
- [7] J. Ko and D. Naidich, "Lung Nodule Detection and Characterization with Multislice CT," *Radiologic Clinics of North America*, Vol. 41, No. 3, pp. 575-597, 2003.
- [8] R. A. Blechschmidt, R. Werthschützky, and U. Lorcher, "Automated CT Image Evaluation of the Lung: A Morphology-Based Concept," *IEEE Trans. on Med. Imaging*, Vol. 20, No 5, pp. 434-442, 2001.
- [9] G. F. Rozin, M. M. Gomes, E. R. Parra, R. A. Kairalla, C. R. R. de Carvalho, and V. L. Capelozzi, "Collagen and elastic system in the remodelling process of major types of idiopathic interstitial pneumonias (IIP)," *Histopathology*, Vol. 46, No. 4, pp. 413-421, 2005.
- [10] I. Cespedes, J. Ophir, H. Ponnekanti, and N. Maklad, "Elastography: elasticity imaging using ultrasound with application to muscle and breast in vivo," *Ultrason. Imaging*, Vol. 15, No. 2, pp. 73-88, 1993.
- [11] J. Ophir, I. Cespedes, B. Garra, H. Ponnekanti, Y. Huang, and N. Maklad, "Elastography: ultrasonic imaging of tissue strain and elastic modulus in vivo," *European J. of Ultrasound*, Vol. 3, No. 1, pp. 49-70, 1996.
- [12] R. M. Lerner, S. R. Huang, and K. J. Parker, "Sonoelasticity Images Derived from Ultrasound Signals in Mechanically Vibrated Tissues," *Ultrasound Med. Biol.*, Vol. 16, No. 3, pp. 231-239, 1990.
- [13] J. Ophir, B. Garra, F. Kallel, E. E. Konofagou, T. A. Krouskop, R. Righetti, and T. Varghese, "Elastographic Imaging," *Ultrasound in Med. & Biol.*, Vol. 26, Supp. 1, pp. S23-S29, 2000.

- [14] T. Shiina, N. Nitta, E. Ueno, and J. C. Bamber, "Real Time Tissue Elasticity Imaging using Combined Autocorrelation Method," *J. Med. Ultrasonics*, Vol. 29, No. 3, pp. 119-128, 2006.
- [15] D. L. G. Hill, P. G. Batchelor, M. Holden, and D. J Hawkes, "Medical Image Registration," *Physics in Medicine and Biology*, Vol. 46, R1-R45, 2001.
- [16] Y. Park, H. Kitaoka, Y. Sato, and S. Tamura, "Matching of 3D Tree Structures Using Association Graph," *J. the Institute of Electronics, Information and Communication Engineers*, Vol. J85-D-II, pp. 1124-1136, 2002.
- [17] Y. Yanagida, S. Kobashi, K. Kondo, and Y. Hata, "Non-rigid registration of multidetector CT images for pulmonary tissue elasticity imaging," *Proc. of World Automation Congress*, pp. 157-162, 2007.
- [18] Y. Yanagida, S. Kobashi, T. Nakano, K. Kondo, Y. Hata, and H. Date, "Automated Lung Lobe Segmentation in MDCT Images with Mixture Information of Lobar Fissures and Tubular Tissue Density," *Proc. of the first Int. Conf. on Complex Medical Engineering*, pp. 341-346, 2005.
- [19] E. H. Mamdani, "Applications of fuzzy algorithms for control of simple dynamic plant," *Proc. of IEEE*, Vol. 121, No. 12, pp. 1585-1588, 1974.

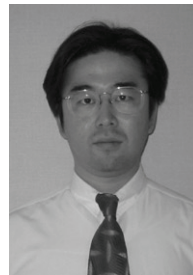
#### AUTHOR INFORMATION



**Syoji Kobashi** received the B.E. (1995), M.E. (1997), and D.E. (2000) degrees from Himeji Institute of Technology, Japan. He is currently an associate professor University of Hyogo. His research interests include soft computing approach to medical image processing and human brain function. He received the Joseph F. Engelberger Best Paper Award from the 2nd World Automation Congress in 2000, and JpCOMPEmbs03 from IEEE EMBS Japan Chapter in 2003. He is a member of IEEE.



**Yosuke Yanagida** received the B.E. degree in 2003 from Himeji Institute of Technology, Japan, and the M.E. degree in 2007 from Univ. of Hyogo, Japan. He was a graduate student of Graduate School of Engineering, Univ. of Hyogo, Japan. He is currently an engineer with To-shiba Medical Systems Corporation, JAPAN. His research interests include medical image processing.



**Katsuya Kondo** received the B.E., M.E., and D.E. degrees from Keio University, Yokohama, Japan, in 1989, 1991 and 1997, respectively. He is an associate professor with University of Hyogo. His research interests include signal processing and computer vision. Dr. Kondo received World Automation Congress Albertos Best Paper Award in 2004. He is a member of the Institute of Electronics, Information and Communication Engineers and IEEE.



**Yutaka Hata** received the B.E. (1984), M.E. (1986), and D.E. (1989) degrees from Himeji Institute of Technology, Japan. He is currently a Professor with University of Hyogo. He now serves as the Chairman of BISC-SIG in Medical Imaging. His research interests include fuzzy logic, medical imaging, ultrasound systems and multiple-valued logic. He received World Automation Congress Contribution Award in 2002 and 2004, Joseph F. Engelberger Best Paper Award and Best Paper Award at the Fourth Biannual World Automated Congress in 2000, and a Distinctive Contributed Paper Award at the IEEE 28th Int. Sympo. on Multiple-Valued Logic from IEEE CS MVL-TC in 1999. He is a senior member of IEEE from 2003.